Post-print version of the manuscript published in

Forest Ecology and Management 464, 118065

https://doi.org/10.1016/j.foreco.2020.118065

Incorporating climate effects in *Larix gmelinii* improves stem taper models in the Greater Khingan Mountains of Inner Mongolia, northeast China

Yang Liu[1, 2], Ralph Trancoso[3], Qin Ma[4], Chaofang Yue[5], Xiaohua Wei[2], Juan A. Blanco[6]*

[1] College of Forestry, Inner Mongolia Agricultural University, Hohhot 010019, China

[2] Department of Earth, Environmental and Geographic Sciences, University of British Columbia (Okanagan), 1177 Research Road, Kelowna, British Columbia V1V 1V7, Canada

E-mail: Yang Liu: liuyangvip@hotmail.com; Xiaohua Wei: adam.wei@ubc.ca

[3] Global Change Institute, University of Queensland, Brisbane, Queensland 4072, Australia
E-mail: ralphtrancoso@gmail.com

[4] Department of Forestry, Mississippi State University, Mississippi State, MS 39762, United States
Email: christine1511@gmail.com

[5] Forest Res Inst Baden Wurttemberg, Wonnhaldestr 4, D-79100 Freiburg, Germany
ChaoFang.Yue@forst.bwl.de

[6] Departamento de Ciencias, Universidad Pública de Navarra, Campus de Arrosadía, Pamplona, Navarra, 31013, Spain
E-mail: juan.blanco@unavarra.es

Corresponding author: Juan A. Blanco

Departamento de Ciencias, Universidad Pública de Navarra, Campus de Arrosadía, Pamplona, Navarra, 31006, Spain
Tel: +34 948 169 859
Fax: +34 948 168 930

E-mail: juan.blanco@unavarra.es

Abstract: Estimating timber volume and carbon stock in forests is fundamental for silviculture and for accurate estimation of national and global carbon budgets. Taper models are important tools for predicting diameter at any height along a tree bole. Mean annual temperature (MAT) and mean annual precipitation (MAP) influence tree growth, but their precise effects on stem shape are still poorly understood and climatic factors are seldom included in taper models. To evaluate the effect of climate on tree stems, we incorporated MAT and MAP as covariates in the Kozak (2004) model to improve model performance in goodness-of-fit. The Kozak (2004) model with the incorporation of MAT and MAP was refitted using nonlinear mixed-effects (NLME) modeling techniques to account for within-sample tree heteroscedasticity and autocorrelation structure in residuals from data measured at different points along the same individual tree stem of *Larix gmelinii* (Rupr.). Results showed that the predictive accuracy of the Kozak (2004) model was improved by incorporating MAT and MAP as covariates. The Kozak (2004) model incorporating both MAT and MAP had the highest prediction accuracy for stem diameter, closely followed by the model incorporating only MAT and then the model incorporating only MAP. MAT effect on tree stem shape was stronger than that of MAP. The NLME Kozak (2004) model incorporating MAT and MAP with exponential variance function and first-order continuous autoregressive correlation structure (CAR(1) model) removed the heteroscedasticity and autocorrelation in the residuals, had the best prediction performance. Therefore, such refined model is recommended for planning and management of natural *L. gmelinii* forests. In conclusion, incorporating the effect of climate variables in stem taper equations could significantly improve timber volume and biomass estimations, particularly in harsh environments, such as natural boreal forests.

Keywords: Variable taper function; Non-linear mixed-effects model; Mean annual temperature; Mean annual precipitation; Stem form

1. Introduction

The forests of the Greater Khingan Mountains cover 30% of China's total forest area (DFPRC, 2014) and play an important role in China´s national carbon budget (Cai *et al.*, 2016). Such forests define the southern boundary of boreal forests in eastern Asia and are dominated by Dahurian larch (*Larix gmelinii* (Rupr.) Rupr.; Editorial Committee for Vegetation of China, 1980). *L. gmelinii* forests contribute more than 20.9% of the total forest area in China (Wang *et al.*, 2001). The volume of *L. gmelinii* forest stock is 0.51 billion m^3 and it accounts for 8% of the national total timber volume (DFPRC, 2014). To reach such stem volume estimations, taper equations are used because these equations can describe the shape of a tree stem by predicting the diameter of the stem at specified heights above the ground. Standing timber volume can then be converted into carbon stocks by using carbon density factors. Therefore, carbon stocks estimated from a suitable taper equation can be used as a scientific basis for boreal forest assessment and management at different scales under the context of managing carbon flows and stocks.

A welcomed group of taper models is variable-form taper equations, which usually have three main advantages: (i) they are flexible and easy to fit, which is important for practical purposes; (ii) they provide a smooth continuous taper profile model; and (iii) they have low multicollinearity (Kozak, 2004). In general, data used for building taper equations are hierarchical or longitudinal data (i.e. diameter measurements on the same stem at different heights, so taper data are not independent but are correlated). Nonlinear mixed-effects models (NLME) including the fixed- and random-effects parameters have been used to model stem taper because they consider heteroscedasticity and autocorrelation among multiple diameter observations on each tree stem (Yang *et al*., 2009). As a consequence, the use of NLME can improve volume and diameter estimation accuracy relative to fixed-effects models (Özçelik *et al*., 2011; Fonweban *et al*., 2012).

Variations in tree taper are affected by several factors, including stand age (Gomat *et al.*, 2011), stand density (Sharma and Parton, 2009), crown variables (Li and Weiskittel, 2010) and management practices, such as thinning treatments (Thomson and Barclay, 1984). Gomat *et al.* (2011) found that dominant trees are more impacted by stand age than suppressed trees. For example, Sharma and Parton (2009) studied the impacts of stand density on the taper equation for jack pine (*Pinus banksiana* Lamb.) and black spruce (*Picea mariana* [Mill.] B. S. P.) in Canada. These authors showed that trees had larger butt diameters and more taper at lower stand density than they did at higher stand density. Incorporating crown variables into

taper equations for primary conifer species in the North American Acadian region demonstrated that these variables could improve prediction accuracy (Li and Weiskittel, 2010). Unfortunately, the ability of crown variables to improve the predictive accuracy of tree profile equations is species-specific (Valentine and Gregoire, 2001), as it is directly related to crown architecture, and therefore generalizations cannot be made. In addition, thinning has been identified as an effective forest treatment to alter tree taper. For example, Thomson and Barclay (1984) reported that when stand density was reduced by heavy thinning, there was more space for the crowns of individual trees to expand and stem butt flare increased, especially in smaller trees.

Climate is directly related to tree mortality through extreme events that can indirectly influence stand density. Previous studies have suggested that climate change (including temperature and water availability) may affect the growth of coniferous forests. For example, at global scale a positive impact of climate change on forest productivity was found when water was not a limiting factor (Boisvenue and Running, 2006). However, forest dieback of *L. gmelinii* has been related to global warming in Siberia (Kobak *et al.*, 1996). Chen *et al.* (2016) also showed increased mortality of mature forests (>40 years old) in Canada due to warming and reduced moisture availability. Generally, forest ecosystems in the mid- to high latitudes may be more sensitive to future climate change in terms of tree growth and expansion, distribution ranges and primary productivity, especially boreal forests (Gang *et al.*, 2017).

In this line, researchers have shown that the boreal forests of the Greater Khingan Mountains, where *L. gmelinii* is the dominant species, are more sensitive to climate change than other Chinese forests (Dai *et al.*, 2002; Wang *et al.*, 2012). The temperature in northeastern China is predicted to increase in the future (Leng *et al.*, 2008). If the temperature increase is <2°C, the population of *L. gmelinii* may decline, and it may be replaced by broadleaf species (He *et al.*, 2005). Bu *et al.* (2008) also predicted that the coverage of *L. gmelinii* could decrease under a warming climate. Precipitation has been shown to affect the growth of *L. gmelinii*, with precipitation influence on *L. gmelinii* growth varying seasonally at high altitudes in the Greater Khingan Mountains (Bai *et al.* (2019). Winter precipitation had a positive effect on growth, whereas summer precipitation had negative impacts on *L. gmelinii* growth at both high- and low-altitude sites.

Although some research has looked at the effects of temperature and precipitation on the growth of *L. gmelinii* in the Greater Khingan Mountains, few studies have examined their effects on the stem taper of *L.*

gmelinii. Knowledge on whether, and how, temperature and precipitation influence the taper of *L. gmelinii* is urgently needed to more accurately estimate the volume and carbon stocks of *L. gmelinii* in the Greater Khingan Mountains under future climate changing conditions. Therefore, we hypothesize that temperature and precipitation can affect tree stem shape by altering growing factors and affect tree architecture. Hence, stem taper equations including climatic factors would provide better estimations of tree volume than regular equations without climatic factors. To test such hypothesis, our aims were: (1) to examine the effect of mean annual temperature (MAT) and mean annual precipitation (MAP) on the tree stem form of *L. gmelinii* in the Greater Khingan Mountains; (2) to modify the variable taper function to incorporate MAT and MAP as independent variables; and (3) to build a nonlinear mixed-effects (NLME) model to account for within-tree heteroscedasticity and autocorrelation in residuals.

2. Materials and Methods

2.1 Climate features in the Greater Khingan Mountains

The Greater Khingan Mountains (Figure 1) are an important climate demarcation line in China, with an increasing temperature gradient (cold-temperate to mid-temperate) from north to south and an increasing humidity gradient (semi-arid to humid) from east to west (Fu *et al.*, 2018). The climate of the Greater Khingan Mountains is a cold temperate continental monsoon with a long cold winter (more than nine months), a short warm summer (less than one month) and a short frost-free period (only 70 to 100 days). The frost sometimes occurs during the growing season in the north part of the mountain chain and at high altitudes. MAT is -2.8°C and the monthly mean temperature has historically varied from -52.3°C in January to 39°C in July. MAP is 442 mm, in which 85% to 90% precipitation occur in summer season (June to August) and 10% precipitation occur from the end of October to the start of April next year, usually as snow. Annual average relative humidity is 70%. The annual snow accumulation period lasts for 5 months, and the depth of snow in the forests is up to 30-50cm (Xu, 1998).

<Figure 1 here>

2.2 Stem data

The data used in this research were collected from natural *L. gmelinii* stands located in the 17 Forestry

Bureaus across the southern, middle and northern sections of the Greater Khingan Mountains, covering the existing range of diameters, heights, stand density and sites for *L. gmelinii* forests (Figure 1). A total of 10,731 measurements were taken from 1,858 felled trees. Tree data were obtained from two sources: (i) 1410 dominant and intermediate trees from 355 plots with areas between 0.04 and 0.32 ha/plot felled between the year of 1985 and 1987, and (ii) 448 trees including dominant, intermediate and suppressed trees from 26 plots with areas from 0.09 to 1.05 ha/plot, felled to model stem shape variability in the year of 2015. Although the measurements were taken in two periods with up to 30 years interval, the method used for taper measurement was relatively consistent. For the total of 1,858 felled *L. gmelinii* trees mentioned above, 20% of the total data were selected at random as a validation dataset (containing 372 trees) using *Sample Function* in R, while the remaining data (containing 1,486 trees) were used for fitting the models (Table 1).

For each tree, the diameter at breast height (DBH) outside bark (D) and diameter outside bark at a height h (d) were measured to the nearest 0.1 cm. Total tree height (H) and height above ground to the measurement point h were measured to the nearest 0.1 m using a tape measure. The lowest measurements of diameter outside bark were taken at stump height between 0.1 and 0.3 m above the ground, then another measurement was usually taken at 0.7 m before reaching the defined breast height of 1.3 m. Measurement intervals above breast height along the stem were 0.5, 1.0 or 2.0 m depending on the height of the sampled tree. Figure 2 shows the variation between the relative height ($q=h/H$) and relative diameter (d/D) according to the measurement data points of the 1,858 trees. Relative height (q) values were divided into ten classes (q intervals of 0.1), within each relative height class, relative diameters are completely independent of each other, which meets the prerequisites of ANOVA. The normality and homogeneity of variances were verified before ANOVA is carried out, respectively, by Shapiro–Wilk and Bartlett values >0.05.

< Figure 2 here>

2.3 Climate data

The climate variables MAT and MAP were observed to be important indicators of climate change in this region (Guo *et al.*, 2013). Thus, MAP and MAT were selected as candidate climate variables in this study. Values for MAT and MAP were calculated from meteorological data recorded by five meteorological stations (Eerguna (EEGN), Genhe (GENH), Yakeshi (YKS), Elunchun (ELC) and Aershan (AES)) located

nearest to the 17 Forestry Bureaus (Figure 1)). The MAT and MAP data for Moerdaoga (MEDG) were obtained from the EEGN meteorological station; MAT and MAP data for Deerbuer (DEBE), Mangui (MG), Alongshan (ALS), Jinhe (JH), and GENH were obtained from the GENH meteorological station; MAT and MAP data for Yitulihe (YTLH), Tulihe (TLH), Kuduer (KDE), and Wuerqihan (WEQH) were obtained from the YKS meteorological station; MAT and MAP data for Ganhe (GH), Alihe (ALH), Keyihe (KYH), and Jiwen (JW) were obtained from the ELC meteorological station; and MAT and MAP data for Chaoyuan (CY), Chaoer (CE), and AES were obtained from the AES meteorological station. The data were downloaded from the China Meteorological Data Service Center (http://data.cma.cn/). The MAT and MAP statistics were averaged for the period 1985–2015. Summary statistics for *D*, *H*, MAT and MAP of sample trees used in fitting and validating the models are described in Table 1.

<Table 1 here>

We used the raw data of the MAT and MAP for each meteorological station to calculate their mean, minimum, maximum and standard deviation. Several time periods were used (5 to 30 years) and potential trends in MAT and MAP over the last 30 years were explored, but as results were not significantly affected by the period selected (results not shown), we decided to use the standard 30 years period for climate normals. Considering these statistics and the actual climatic conditions in the Greater Khingan Mountains, we classified the MAT and MAP into three different classes: <400 mm, 400 to 450 mm, and >450 mm (for MAP); and <−3.0°C, −3.0 to −2.0°C, and >−2.0°C (for MAT) to analyze whether d/D were statistically different among MAT and MAP classes using the univariate analysis of variance (ANOVA). As with relative diameters, normality and homogeneity of variances were verified before ANOVA is carried out, respectively, by Shapiro–Wilk and Bartlett values >0.05.

2.4 Model analysis and development

We first compared ten variable-form taper models, and evaluated their performances based on statistical indicators of fit and validation. The Kozak (2004) variable-exponent model, which showed a larger adjusted coefficient of determination (R^2_{adj}), and smaller root mean squared error (RMSE), mean absolute error

(MAE) and mean percentage of relative bias (MPRB) than the other models, was selected as the foundation model in this study for further analysis in predicting diameters at any height along the tree bole for *L. gmelinii*. The form of the most accurate Kozak (2004) model is:

$$d_{sij} = b_1 D_{si}^{\,b_2} H_{si}^{\,b_3} x_{sij}^{\left[b_4 q_{sij}^4 + b_5\left[1/e^{D_{si}/H_{si}}\right] + b_6 x_{sij}^{0.1} + b_7(1/D_{si}) + b_8 H_{si}^{(1-q_{sij}^{1/3})} + b_9 x_{sij}\right]} + \varepsilon_{sij} \qquad (1)$$

where d_{sij} (cm) is diameter outside bark at a height h_{sij} of the j^{th} measurement in the i^{th} tree in the s^{th} meteorological station; D_{si} (cm) and H_{si} (m) are the DBH outside bark and total tree height of the i^{th} tree in the s^{th} meteorological station; $q_{sij} = h_{sij}/H_{si}$ is relative height, $x_{sij} = (1-q_{sij}^{1/3})/(1-(1.3/H_{si})^{1/3})$; ε_{sij} is an error term; and $b_{i...n}$ are the regression coefficients.

Because the exponent of the height solely determines the overall shape of a tree (Sharma and Zhang, 2004), the original Kozak (2004) model can be modified to accommodate the effects of climate on the taper of *L. gmelinii* by adding the MAT and/or MAP to the exponent to further improve model precision. Modifying the exponents for *D* and *H* due to MAP and MAT would have a similar effect on taper along the whole stem, while modifying the exponent for variable *x* allows the effect of MAP and MAT on taper to vary along the stem. We chose the three optional linear terms: (1) b_{10}MAT, (2) b_{10}MAP, and (3) b_{10}MAT+b_{11}MAP in the exponent of *x* because it allowed the greatest flexibility in capturing variability along the stem. Preliminary analyses showed that the interaction between MAP and MAT did not exert significant effects on *d*, which can be expressed as b_{10}MAT*MAP, b_{10}MAP+ b_{11}MAT*MAP and b_{10}MAT+ b_{11}MAT*MAP (data not shown). Hence, three Kozak (2004) models with climate variables included as a predictor in the exponent were defined as follows:

$$d_{sij} = b_1 D_{si}^{\,b_2} H_{si}^{\,b_3} x_{sij}^{\left[b_4 q_{sij}^4 + b_5\left[1/e^{D_{si}/H_{si}}\right] + b_6 x_{sij}^{0.1} + b_7(1/D_{si}) + b_8 H_{si}^{(1-q_{sij}^{1/3})} + b_9 x_{sij} + b_{10}\mathrm{MAP}_{si}\right]} + \varepsilon_{sij} \qquad (2)$$

$$d_{sij} = b_1 D_{si}^{\,b_2} H_{si}^{\,b_3} x_{sij}^{\left[b_4 q_{sij}^4 + b_5\left[1/e^{D_{si}/H_{si}}\right] + b_6 x_{sij}^{0.1} + b_7(1/D_{si}) + b_8 H_{si}^{(1-q_{sij}^{1/3})} + b_9 x_{sij} + b_{10}\mathrm{MAT}_{si}\right]} + \varepsilon_{sij} \qquad (3)$$

$$d_{sij} = b_1 D_{si}^{\,b_2} H_{si}^{\,b_3} x_{sij}^{\left[b_4 q_{sij}^4 + b_5\left[1/e^{D_{si}/H_{si}}\right] + b_6 x_{sij}^{0.1} + b_7(1/D_{si}) + b_8 H_{si}^{(1-q_{sij}^{1/3})} + b_9 x_{sij} + b_{10}\mathrm{MAT}_{si} + b_{11}\mathrm{MAP}_{si}\right]} + \varepsilon_{sij} \qquad (4)$$

where d_{sij} (cm) is diameter outside bark at a height h_{sij} of the j^{th} measurement in the i^{th} tree in the s^{th} meteorological station; D_{si} (cm) and H_{si} (m) are the DBH outside bark and total tree height of the i^{th} tree in the s^{th} meteorological station; $q_{sij} = h_{sij}/H_{si}$, $x_{sij} = (1-q_{sij}^{1/3})/(1-(1.3/H_{si})^{1/3})$; MAT_{si} and MAP_{si} are mean annual

temperature and mean annual precipitation corresponding to the s^{th} (s=1, 2, 3, 4, 5) meteorological station in which the i^{th} tree is located, respectively; ε_{sij} is an error term; and $b_{i...n}$ are parameters.

2.5 NLME model

Using a nonlinear mixed-effects (NLME) model (Davidian and Giltinan, 1995), the selected best Kozak (2004) model incorporating climate variables can be expressed as follows:

$$\mathbf{d}_i = f(\boldsymbol{\beta}, \mathbf{u}_i, \mathbf{X}_i) + \boldsymbol{\varepsilon}_i \qquad \boldsymbol{\varepsilon}_i \sim N(0, \mathbf{R}_i) \qquad \mathbf{u}_i \sim N(0, \mathbf{D}) \tag{5}$$

where $\mathbf{d}_i$ is the vector of diameter outside bark at the different heights h on the i^{th} tree; $\mathbf{X}_i$ is the vector for independent variables; $\boldsymbol{\beta}$ is the vector of fixed-effects parameters; $\mathbf{u}_i$ is the vector of random effects for sample tree i; N is the multivariate normal distribution; $\mathbf{D}$ is the variance–covariance structure matrix; $\boldsymbol{\varepsilon}_i$ is random error; $\mathbf{R}_i$, which needs to be specified to account for any within-tree heteroscedasticity and autocorrelation among measurements, is the within-tree variance–covariance matrix and is expressed as follows:

$$\mathbf{R}_i = \sigma^2 \mathbf{G}_i^{0.5} \boldsymbol{\Gamma}_i \mathbf{G}_i^{0.5} \tag{6}$$

where σ^2 is a scaling factor for error dispersion which is given by the value of residual variance of the estimated model; $\mathbf{G}_i$ is the diagonal matrix explaining the variance of within-tree heteroscedasticity; and $\boldsymbol{\Gamma}_i$ is a matrix accounting for the within-tree autocorrelation structure of the errors. The heteroscedasticity errors and autocorrelation errors exist widely in the repeated diameter measurements on the same tree.

Preliminary analyses showed that the first-order continuous autoregressive correlation structure (CAR(1) models) can best model the autocorrelation within the sample tree, which can be expressed as $\mathrm{Cov}(\varepsilon_j, \varepsilon_{j'}) = \rho^{d_{jj'}}$, where $\mathrm{Cov}(\varepsilon_j, \varepsilon_{j'})$ is the covariance of two model residuals ε_j and $\varepsilon_{j'}$ for two diameter values from the sample tree i; ρ is the estimated parameter of CAR(1); $d_{jj'} = |h_{ij} - h_{ij'}|$, for $j \neq j'$ is the distance between two observed h on the sample tree i (Pinheiro and Bates, 2000). The increasing within-tree heteroscedasticity with predicted diameter outside bark can be best modeled using the exponential of the fitted value ($\hat{\mathrm{d}}$) variance function, which can be expressed as $\mathrm{Var}(\varepsilon_i) = \sigma^2 \exp(2\delta \hat{\mathrm{d}}_i)$, where σ^2 is the value of residual variance of the estimated model, and δ are estimated parameters. The above-described within-group

correlation structure (CAR(1) models) and within-group heteroscedasticity structure (exponential variance function) in this study, respectively, showed the smallest fit evaluation criteria: that is, Akaike´s information criterion (AIC) and Bayesian information criterion (BIC) (Schwarz, 1978; Sakamoto *et al.*, 1986).

D is the variance–covariance matrix for the random-effects parameters $\mathbf{u}_i$, which explains between-tree random variability, generally assumed to be the unstructured positive definite matrix in tree profile research (Yang *et al.*, 2009). We used our tree profile data also to find the smallest AIC and BIC when the **D** matrix is considered to be the unstructured positive definite matrix.

To determine the parameter types (fixed effects or fixed plus random effects) of the NLME model, the different combinations of the parameter types for the selected best Kozak (2004) model incorporating climate variables in this study were evaluated with the method applied by Trincado and Burkhart (2006). The best model was selected using AIC, BIC, and twice the negative log-likelihood (−2Ln(L)). The parameters of NLME models were estimated using restricted maximum likelihood with the *nlme* function of the nlme package in R (Pinheiro *et al.*, 2018).

The sample tree-level random effects parameters $\hat{\mathbf{u}}_i$ were calculated using the empirical best linear unbiased prediction (EBLUP) method (Vonesh and Chinchilli, 1997). The expression is as follows:

$$\hat{\mathbf{u}}_i = \hat{\mathbf{D}}\hat{\mathbf{Z}}_i^T(\hat{\mathbf{R}}_i + \hat{\mathbf{Z}}_i\hat{\mathbf{D}}\hat{\mathbf{Z}}_i^T)^{-1}\hat{\mathbf{e}}_i \quad (7)$$

where $\hat{\mathbf{u}}_i$ is the estimated random effects parameter for sample tree *i*; $\hat{\mathbf{D}}$ is the estimated variance-covariance matrix for $\mathbf{u}_i$; $\hat{\mathbf{R}}_i$ is the estimated within-tree variance–covariance matrix for $\boldsymbol{\varepsilon}_i$; $\hat{\mathbf{e}}_i = \mathrm{d}_i - f(\mathrm{X}_i, \beta, 0)$ is the residuals vector, which is calculated by subtracting the estimated d_i using the fixed-effects model from the observed d_i of the sample tree *i* for the subsample; *f*(.) is a nonlinear function of the independent variable $\mathbf{X}_i$; and $\hat{\mathbf{Z}}_i$ is the design matrix of the partial derivatives of $\mathbf{Z}_i = \left.\frac{\partial f(\boldsymbol{\beta}, \mathbf{u}_i, \mathbf{X}_i)}{\partial \mathbf{u}_i}\right|_{\hat{\boldsymbol{\beta}}, \mathbf{u}_i=0}$. Details of random-effects parameters estimation for the NLME model in forestry were introduced in Fang and Bailey (2001) and Calama and Montero (2004).

2.6 Model evaluation

To evaluate the fit and prediction performance of fixed- and mixed-effects models, several criteria and

the standardized residual plots were applied. For these criteria, besides AIC and BIC, the R^2_{adj} (the fit indicator, Eq. (8)), RMSE (Eq. (9)), MAE (Eq. (10)) and MPRB (Eq. (11)) (Li and Weiskittel, 2010) were also calculated for both fitting and validation (independent) datasets. The corresponding expression is as follows:

$$R^2_{adj} = 1 - \frac{(n-1)\cdot\sum_{i=1}^{n}(y_i - \hat{y}_i)^2}{(n-p-1)\cdot\sum_{i=1}^{n}(y_i - \bar{y}_i)^2} \quad (8)$$

$$RMSE = \sqrt{\sum_{i=1}^{n}(y_i - \hat{y}_i)^2 / n - p} \quad (9)$$

$$MAE = \sum_{i=1}^{n}\left|y_i - \hat{y}_i\right| / n \quad (10)$$

$$MPRB = \sum_{i=1}^{n}\left|y_i - \hat{y}_i\right| / \sum_{i=1}^{n} y_i \times 100\% \quad (11)$$

where y_i is the observed value of the diameter for the *i*th observation, $\hat{y}_i$ is the predicted value of the diameter for the *i*th observation, $\bar{y}_i$ is the mean value of the y_i, n is the number of observations in the fitting or valuation dataset, and p is the number of estimated parameters in the corresponding stem taper model.

3 Results

3.1 Impact of MAP and MAT on stem taper

There were significant differences in the relative diameter of the trees among the three MAP and MAT classes along the entire tree stem ($0<q\leq1$; F=213.2 and 171.3, $p<0.001$; Tables 2 and 3). The relative diameter (*d/D*) increased with higher MAP (Table 2). The relative diameter of the tree bole in the stands with MAP larger than 450 mm was up to 1.2 times greater than those stands with MAP smaller than 400 mm. The average relative diameter of a tree bole in the stands with MAT lower than −3.0 was 0.665 ± 0.009, significantly lower than the other two stands with MAT between −3.0 and −2.0°C and MAT larger than −2.0°C ($p<0.001$, Table 3). For the three MAP and three MAT classes, there were significant differences for the average relative diameter among ten different relative height classes (q intervals of 0.1), except for that of $0.1<q\leq0.2$ and $0.2<q\leq0.3$ (for the three MAP classes), and except for that of $0.2<q\leq0.3$ and $0.3<q\leq0.4$ (for the three MAT classes), where stem forms were generally modeled geometrically as a cylindrical shape (q ranges from 0.1 to 0.4). Similar to the cylindrical shape, there was no effect of MAP and MAT on the average relative diameter

of a tree bole where tree stems were modeled as conical frustums ($0.9<q<1$). Overall, the ANOVA indicated that MAP and MAT generally had significant effects on the tree stem diameter ($p<0.001$). Thus, MAP and MAT were incorporated into the Kozak (2004) model as predictors to improve the accuracy of taper equations for *L. gmelinii*.

<Table 2 here>

<Table 3 here>

3.2 Analysis of the tree profile equation incorporating climate variables

The parameters for the Kozak (2004) model, which were significant at the 95% confidence level in the models incorporating MAP or/and MAT (Eqs. 2–4), are reported in Table 4. Based on the diagram of stem profile simulation (Figure 3) and the evaluation statistics of the three analyzed taper models (Eqs. 2–4) (Table 5), the Kozak (2004) model with MAP and MAT was rated as the best among the three candidate models, followed by the Kozak (2004) model with MAT, and finally by the Kozak (2004) model with MAP. This indicated that the impact of climate variables on the stem form decreased in the order: adding both MAP and MAT (reducing MAE 5.5%) > adding only MAT (reducing MAE 4.1%) > adding MAP only (reducing MAE 2.8%). The incorporation of MAT and MAP simultaneously into the Kozak (2004) model led to the lowest AIC (Table 4), when compared with the Kozak (2004) models that incorporated MAT alone or MAP alone and the Kozak (2004) model without MAT and MAP. Therefore, we selected the Kozak (2004) model with MAP and MAT (Eq. (4)) as the optimal model to develop the NLME taper models.

<Table 4 here>

<Table 5 here>

< Figure 3 here>

3.3 NLME taper models and their parameter estimates

Among all possible combinations of random effects and fixed effects for Eq. (4), the best combination of the converged models selected b_2 and b_8 as mixed effects parameters. This combination gave the lowest AIC value (25049.5) and BIC value (25155.4), and the largest log likelihood values (−12509.8). The final NLME model (Eq. (12)), including the random effects parameters, was:

$$d_{sij} = b_1 D_{si}^{(b_2+u_{2i})} H_{si}^{b_3} x_{sij}^{\left[b_4 q_{sij}^4 + b_5\left[1/e^{D_{si}/H_{si}}\right] + b_6 x_{sij}^{0.1} + b_7(1/D_{si}) + (b_8+u_{8i}) H_{si}^{(1-q_{sij}^{1/3})} + b_9 x_{sij} + b_{10}\mathrm{MAT}_{si} + b_{11}\mathrm{MAP}_{si} \right]} + \varepsilon_{sij} \quad (12)$$

where u_{2i} and u_{8i} are the random-effects parameters produced by the i^{th} sample tree on b_2 and b_8, respectively.

The model parameters and variance components for Eq. (12) are shown in Table 4. All parameters were significant at the 95% confidence level. However, the combination of b_2 and b_8 as mixed effects parameters (random effects parameters related to the sample tree) and other parameters as fixed effects was not enough to eliminate the heteroscedasticity and autocorrelation because the AIC difference (up to 10%) between Eq. (12) and Eq. (12) with exponential variance functions and CAR(1) model was significant (Table 4). The likelihood ratio tests also showed significantly improvements to the performance of Eq. (12) (using L.Ratio=2402.5, p<0.0001), when simultaneously including the exponential variance function to model the heteroscedasticity and the CAR(1) model to remove the autocorrelation within the sample tree (the Eq. (12) with exponential variance functions and CAR(1) model). The estimated residual variance σ^2 values decreased from 1.36189 to 0.30491 (reduction of 77.6%). The Eq. (12) with exponential variance functions and CAR(1) model showed much better goodness of fit measures than the other five models (Table 4).

3.4 Predicted diameters and model calibration

The difference between fixed and mixed effects models is that mixed effects models require prior measured diameter information, but fixed effects models do not. In this study, four randomly selected prior measurements of the upper stem diameters from each tree were used to estimate the random effects of NLME models and also to calibrate diameters and calculate the evaluation statistics for the NLME models. This procedure was suggested by Fu *et al.* (2017). All the evaluation statistics for the fitting and validation datasets for the fixed and mixed effects taper models are shown in Table 5. The Eqs. 1 to 4 and Eq. 12 with exponential variance function and CAR(1) model explained more than 97.9% of the entire stem taper variation. Based on the fitting and validation statistics, plus the diameter outside bark standardized residuals plot (Figure 4), the Eq. 12 with exponential variance function and CAR(1) model showed the best results in estimating d, which further reduced the MAE by 2.8%–8.0% and 3.4%–10.2% for the fitting and validation datasets, respectively, when compared with the other four fixed effects taper equations (Table 5).

The differences in RMSE among the five models were at most 8.2%. The d predictions for 10 relative

height classes were further evaluated using the evaluation statistics of validation datasets for Eq. 1, Eq. 4 and Eq. 12 with exponential variance function and CAR(1) model (Table 6). The diameter predictions were better for middle stems than lower and upper stems for all the three models. The Kozak (2004) model (Eq. 1) with observed bottom ($0<q\leq0.1$) and upper ($0.7<q\leq1.0$) stem diameters performed quite well in terms of RMSE, MAE and MPRB. However, Eq. 12 with exponential variance function and CAR(1) model provided a more accurate prediction of stem diameters for lower and middle sections ($0.1<q\leq0.7$) based on the evaluation statistics (Table 6). As relative diameter became greater, relative tree height (q) became smaller. The standardized residuals of diameter in the sections with relative diameter classes ranging from 0.1 to 1.0 were reduced for Eq. 12 with exponential variance function and CAR(1) model, particularly for sections with relative diameters ranging from 0.6 to 1.0 (Figure 4). The standardized residuals were slightly positive for the lowest of the stems with relative diameter of 1.3 in the Kozak (2004) model (Eq. 1) and Kozak (2004) model with MAP and MAT, but became slightly negative in the Eq. 12 with exponential variance function and CAR(1) model (Figure 4). In summary, the mixed-effects model had the lowest bias for the upper stem diameter predictions, closely followed by the Kozak (2004) model incorporating MAP and MAT and then by the Kozak (2004) model.

<Table 6 here>

< Figure 4 here>

4. Discussion

4.1. Influence of temperature and precipitation on stem shape

Taper models can be used to predict the relationship between tree growth, timber volume and carbon stocks (Fonweban *et al.*, 2011). Our results support our initial hypothesis, as they indicate that climate-related factors significantly affect tree shape. Our study also showed that the Kozak (2004) model incorporating climate was significantly better than other models for predicting stem diameter. This result is consistent with that of Rojo *et al.* (2005), who evaluated the performance of 31 well-known taper models and found that the Kozak (2004) model was more accurate than the next best performing model. Heiðarsson and Pukkala (2011) and Corral-Rivas *et al.* (2007) also suggested that the Kozak (2004) model was the most suitable for predicting diameters along the stem for both Siberian larch (*L. sibirica*) and lodgepole pine (*P. contorta*) in Iceland, and

another five pine species analyzed in El Salto Durango (Mexico), respectively. In Canada, the Kozak (2004) model is extensively used to predict the diameter of the stem and individual tree volume for major tree species in British Columbia (Nigh and Smith, 2012) and Alberta (Yang *et al.,* 2009). These studies suggest that although taper equations are generally species-specific, the Kozak (2004) model can be successfully used to estimate diameter in many different tree species because it is highly flexible (Kozak, 2004). Therefore, improving such model with climate-dependent variables could have applicability in a wide range of forest types.

In addition, our results show that stem form is not only influenced by biotic factors (e.g. stand density, age, tree species, stand origin and branch location), but also impacted by abiotic factors (e.g. climate variable and site characteristics) (Meng, 2006). Although the Kozak (2004) model has been shown to successfully predict stem diameters, the effect of climate variables on the stem taper of *L. gmelinii* is significant and it should be incorporated into the model structure as covariates to further increase the accuracy of existing the Kozak (2004) model. The climate factors (MAT and MAP) have important impacts on taper, which is consistent with the finding of Chen *et al.* (2016), who showed that temperature and moisture availability affected the net biomass of boreal forests in western Canada. Schneider *et al.* (2018) also reported that the taper of white birch (*Betula papyrifera* Marsh.) decreased with increasing summer temperatures and winter precipitation in the province of Quebec, Canada.

MAP and MAT should be considered as surrogates for a summary of several environmental factors interconnected among them. For example, MAT depends on both elevation and orientation, with mountaintops and northern-facing slopes being colder and therefore having shorter growing seasons. This could be translated into stems growing slowly in diameter, particularly in the top sections, and stems becoming more conical. MAT could also be related to topography, as lower temperatures are usually combined with steeper slopes that could force swollen butts to increasing structural stability. Similarly, MAP is usually higher as altitude increases, but in this region that is translated into more snow loads and stronger winds, which again could force a more conical stem shape to increase stability against snow and wind damage.

The MAT and MAP were simultaneously included in the Kozak (2004) model (Eq. (4)) as predictors, which gave better results than models that either only included MAT (Eq. (2)) or MAP (Eq. (3)) in estimating tree diameters at any height. The additional climate variables improved the model performance more for MAT than MAP by reducing MAE by 4.1% and 2.8%, respectively. Therefore, MAT was the main climate factor

influencing *L. gmelinii* taper in the Greater Khingan Mountains. This result is consistent with Guo *et al.* (2019), who found that MAT was the most important driver for stem growth in Asian boreal forests. Other studies showed that temperature was the key climate factor driving the growth of trees in cold alpine regions (Pauli *et al.*, 2012; Suvanto *et al.*, 2016b). We have also found that temperature had a positive effect on relative diameter. When the temperature was higher than −2.0 °C, the relative diameter (0.803±0.002) was larger than that of other MAT classes (Table 3). This result corroborates the positive relationship between temperature and stem diameter reported for *L. gmelinii* taper in the Greater Khingan Mountains by Jiang *et al.* (2016).

Under warmer temperatures, trees in the boreal latitudes tend to develop more wood cells in wider shape, causing higher annual diameter growth (Lo *et al.*, 2010), which translates into the significant positive relationship between temperature and stem shape shown by our results. Such positive temperature-diameter relationships are widely documented in dendroclimatological research (Hughes *et al.*, 2011). On the other hand, in natural even-aged stands tree height growth is less directly related to competition among trees than diameter growth. Under these conditions, top height variations across sites mainly depend on environmental factors, and top height traditionally serves as a proxy for site fertility in forestry (Skovsgaard and Vanclay, 2008). In northern latitudes, it has been shown that boreal tree height is more dependent on temperature than precipitation, being spring temperatures particularly influential on tree height growth (Bloom *et al.*, 1985; Messaoud and Chen, 2011). Therefore, our results showing a stronger influence of temperature than precipitation on tree shape, which are consistent with previous research for boreal forests. However, as tree stem growth is a cumulative process of annual increments during many years and therefore it has an important legacy from previous years, our results should be interpreted that if MAT and MAP change at these sites, new tree generations will have different stem shape from the trees historically harvested from the Greater Khingan Mountains or the mature tree still standing.

4.2. Predictive performance of taper equations with climate factors

The relative height (q) was divided into ten sections to evaluate the predictive performance of the models along the whole stem. The Kozak (2004) model (Eq. 1) with observed bottom ($0<q\leq0.1$) and upper ($0.7<q\leq1.0$) stem diameters performed the best in terms of RMSE and MAE. However, the Eq. 12 with exponential variance function and CAR(1) model provided the best prediction of upper stem diameters for lower and middle sections

($0.1<q\leq0.7$) based on the evaluation statistics (Table 6 and Figure 4). Similar results were reported by Özçelik *et al.* (2011) and Yang *et al.* (2009): in other words, the NLME model showed the highest precision for the lower and middle stem sections compared with the fixed-effects model with and without other predictor variables. This result could be explained as the NLME tree profile equations with exponential variance function and CAR(1) model were successful at removing the heteroscedasticity and autocorrelation in model residuals, which are caused by multiple measurements of an individual tree (Yang *et al.*, 2009; Li and Weiskittel, 2010). However, the NLME created bias with estimation for small (at the relative height of $0.7<q\leq1.0$) and large (at the relative height of $0<q\leq0.1$) relative diameters, i.e., such issue could lead to poor predictive performance for the upper and bottom stem diameters, being of particular importance for those trees growing in natural forests in harsh environments, such as *L. gmelinii* in the Greater Khingan Mountains.

Stem diameter predictions were less precise for the stem section of small relative diameter, which may be caused by an over-prediction of the calibrated diameters for that relative height class ($0.7<q\leq1.0$), as this location is closer to the tree top with fairly small diameters in general (Yang *et al.*, 2009). Similar conclusions were reached by Trincado and Burkhart (2006) and Özçelik *et al.* (2011), when using the NLME modeling technique. The poor predictions at the bottom section for the NLME model (RMSE was employed as a primary criterion for model evaluation) may be due to the butt swell presented by *L. gmelinii* trees at that relative height class, $0<q\leq0.1$, when compared with predictions based only on fixed-effects models. Even though the NLME model can remove part of the heteroscedasticity and autocorrelation in the residuals, it has often been shown to predict butt sections poorly. In spite of that, the butt error may be of little practical significance because this height, which corresponds closely to stump height, is not the main timber portion and is usually not harvested but left on site (Fonweban *et al.*, 2011). Similar cases of poor predictive performance for the butt sections by taper modeling were reached by Fonweban *et al.* (2011) and Parresol *et al.* (1987). It has also been reported that harsh environments produce shorter trees (Marks *et al.*, 2016), due the limited resource for growing and also the need to adapt to perturbances, such as winter storms with high winds and heavy snow loads. Such shorter tree stems have more taper to develop stronger roots, which are critical to anchoring boreal trees against winter storms (Suvanto *et al.*, 2016a). Therefore, such shorter trees tend to develop larger butt diameter (Danquechin Dorval *et al.*, 2016).

Supporting this argument, the ANOVA results also demonstrated that there was no impact of either MAP

or MAT on the average relative diameter of the tree bole near the top of the stem ($0.9<q<1$). This result could be because the vertical-axis system produces vigorous growth at the top of the tree and, therefore, the shape of the bole shows a sharp change. Alternatively, this could be caused by an overestimation of *d* for that relative height class ($0.7<q\leq1.0$). Because this location is closer to the top of the stems with relatively small diameters in general, the effect of the sample tree-level random effects on *d* should be small. However, the Kozak (2004) model with MAP and MAT showed consistent performance for each section and exhibited only moderate variation in any section, which indicated that the inclusion of climate variables improved the performance of the stem form model in this study. Our results are also aligned with previous findings on the importance of climate on stem shape in European forests (Fortin *et al.*, 2019), and follow Kimmins *et al.* (2008) indications that forest models should be simple, but include all the factors relevant for estimating the target variable.

Our work indicates possibilities for further research to keep increasing the accurate estimation of diameter, volume, biomass or carbon in standing forests as well as in harvested trees. In this study, the regional climate differences exerted significant effects on the stem taper was explored. However, the appropriate temporal frame for climate differences of that is most correlated with tree form during the monitoring years could not be found as only data from two harvesting events were available. In future work, the continuous observation of stem data (with dendrometers of dendrochronological samples) could be used to carry out to study potential lag effects and therefore determine the appropriate temporal frame of climate differences that is most correlated with tree form at the time of measurement using the dynamic modeling.

5. Conclusions

The flexibility of the Kozak (2004) model demonstrates acceptable predictive accuracy for stem diameter and can be adapted to simulate the taper profile of *L. gmelinii* in the Greater Khingan Mountains of Inner Mongolia, northeast China. The Kozak (2004) model including MAT and/or MAP showed a significant improvement on predictions of stem diameter. The NLME approach was used to fit the stem taper equations. The heteroscedasticity and autocorrelation in the residuals were modeled by the exponential variance function and CAR(1) model. Based on our results, the NLME Kozak (2004) model including MAT and MAP is recommended for the estimation of diameter at specific heights of *L. gmelinii* stem when upper stem diameter measurements are available. To our knowledge, very few previous attempts have been made to demonstrate

the effect of climate on taper, and even fewer studies have developed specific stem taper equations that included climate variables as covariates for *L. gmelinii*. In these boreal forests, climate plays a role in stem shape (through improving stem growth in height and diameter when conditions are favorable and through the selection of trees well rooted and better able to resist mechanical loads from snow and wind). This study will improve the prediction accuracy of tree-specific diameters at any height along the tree bole and make up for the deficiencies of previous regional taper equations in the Greater Khingan Mountains, particularly in the context of changing climate that could affect tree shape.

Acknowledgements

This study was funded by the Transformation Project of Science and Technology Result of Inner Mongolia Autonomous Region (CGZH2018058) and Excellent Young Scientist Foundation of Inner Mongolia Agricultural University of China (No. 2014XYQ-6). The authors declare that they have no conflict of interests. We would also like to thank all anonymous reviewers for their valuable suggestions.

References

Bai, X., Zhang, X., Li, J., Duan, X., Jin, Y., Chen, Z., 2019. Altitudinal disparity in growth of Dahurian larch (Larix gmelinii Rupr.) in response to recent climate change in northeast China. Sci. Total Environ. 670, 466-477.http://dx.doi.org/10.1016/j.scitotenv.2019.03.232.

Bloom, A.J., Chapin, F.S., Mooney, H.A., 1985. Resource Limitation in Plants-An Economic Analogy. Annu. Rev. Ecol. Syst. 16, 363-392.http://dx.doi.org/10.1146/annurev.es.16.110185.002051.

Boisvenue, C., Running, S.W., 2006. Impacts of climate change on natural forest productivity – evidence since the middle of the 20th century. Global Change Biol. 12, 862-882.http://dx.doi.org/10.1111/j.1365-2486.2006.01134.x.

Bu, R., He, H.S., Hu, Y., Chang, Y., Larsen, D.R., 2008. Using the LANDIS model to evaluate forest harvesting and planting strategies under possible warming climates in Northeastern China. For. Ecol. Manage. 254, 407-419.http://dx.doi.org/10.1016/j.foreco.2007.09.080.

Cai, H., Di, X., Chang, S.X., Wang, C., Shi, B., Geng, P., Jin, G., 2016. Carbon storage, net primary production, and net ecosystem production in four major temperate forest types in northeastern China. Can. J. For. Res. 46, 143-151.http://dx.doi.org/10.1139/cjfr-2015-0038.

Calama, R., Montero, G., 2004. Interregional nonlinear height-diameter model with random coefficients for stone pine in Spain. Can. J. For. Res. 34, 150-163.http://dx.doi.org/10.1139/x03-199.

Chen, H.Y.H., Luo, Y., Reich, P.B., Searle, E.B., Biswas, S.R., 2016. Climate change-associated trends in net biomass change are age dependent in western boreal forests of Canada. Ecol. Lett. 19, 1150-1158.http://dx.doi.org/10.1111/ele.12653.

Corral-Rivas, J.J., Diéguez-Aranda, U., Corral Rivas, S., Castedo Dorado, F., 2007. A merchantable volume system for major pine species in El Salto, Durango (Mexico). For. Ecol. Manage. 238, 118-129.http://dx.doi.org/10.1016/j.foreco.2006.09.074.

Dai, L., Wu, G., Zhao, J., Kong, H., Shao, G., Deng, H., 2002. Carbon cycling of alpine tundra ecosystems on Changbai Mountain and its comparison with arctic tundra. Science in China, Series D: Earth Sciences 45, 903-910.http://dx.doi.org/10.1360/02yd9089.

Danquechin Dorval, A., Meredieu, C., Danjon, F., 2016. Anchorage failure of young trees in sandy soils is prevented by a rigid central part of the root system with various designs. Ann. Bot. 118, 747-762.http://dx.doi.org/10.1093/aob/mcw098.

Davidian, M., Giltinan, D.M., 1995. Nonlinear models for repeated measurement data. Chapman & Hall, London.

DFPRC, 2014. Statistics of China's Forest Resources (2009-13), Department of Forestry of PR China, Beijing, China.

Editorial Committee for Vegetation of China, 1980. Vegetation of China. Science Press, Beijing, China.

Fang, Z., Bailey, R.L., 2001. Nonlinear Mixed Effects Modeling for Slash Pine Dominant Height Growth Following Intensive Silvicultural Treatments. For. Sci. 47, 287-300.http://dx.doi.org/10.1093/forestscience/47.3.287.

Fonweban, J., Gardiner, B., Auty, D., 2012. Variable-top merchantable volume equations for Scots pine (Pinus sylvestris) and Sitka spruce (Picea sitchensis (Bong.) Carr.) in Northern Britain. Forestry 85, 237-253.http://dx.doi.org/10.1093/forestry/cpr069.

Fonweban, J., Gardiner, B., Macdonald, E., Auty, D., 2011. Taper functions for Scots pine (Pinus sylvestris L.) and Sitka spruce (Picea sitchensis (Bong.) Carr.) in Northern Britain. Forestry 84, 49-60.http://dx.doi.org/10.1093/forestry/cpq043.

Fortin, M., Van Couwenberghe, R., Perez, V., Piedallu, C., 2019. Evidence of climate effects on the height-diameter relationships of tree species. Ann. For. Sci. 76, 1.http://dx.doi.org/10.1007/s13595-018-0784-9.

Fu, L., Zhang, H., Sharma, R.P., Pang, L., Wang, G., 2017. A generalized nonlinear mixed-effects height to crown base model for Mongolian oak in northeast China. For. Ecol. Manage. 384, 34-43.http://dx.doi.org/10.1016/j.foreco.2016.09.012.

Fu, Y., He, H.S., Zhao, J., Larsen, D.R., Zhang, H., Sunde, M.G., Duan, S., 2018. Climate and Spring Phenology Effects on Autumn Phenology in the Greater Khingan Mountains, Northeastern China. Remote Sens. 10, 449.http://dx.doi.org/10.3390/rs10030449.

Gang, C., Zhang, Y., Wang, Z., Chen, Y., Yang, Y., Li, J., Cheng, J., Qi, J., Odeh, I., 2017. Modeling the dynamics of distribution, extent, and NPP of global terrestrial ecosystems in response to future climate change. Global Planet. Change 148, 153-165.http://dx.doi.org/10.1016/j.gloplacha.2016.12.007.

Gomat, H.Y., Deleporte, P., Moukini, R., Mialounguila, G., Ognouabi, N., Saya, A.R., Vigneron, P., Saint-Andre, L., 2011. What factors influence the stem taper of Eucalyptus: growth, environmental conditions, or genetics? Ann. For. Sci. 68, 109-120.http://dx.doi.org/10.1007/s13595-011-0012-3.

Guo, W.-L., Hong-Bo, S., Jing-Jin, M., Ying-Juan, Z., Ji, W., Wen-Jun, S., Zi-Yin, Z., 2013. Basic Features of Climate Change in North China during 1961–2010. Adv. Clim. Change Res. 4, 73-83.http://dx.doi.org/10.3724/SP.J.1248.2013.073.

Guo, Y., Peng, C., Trancoso, R., Zhu, Q., Zhou, X., 2019. Stand carbon density drivers and changes under future climate scenarios across global forests. For. Ecol. Manage. 449, 117463.http://dx.doi.org/10.1016/j.foreco.2019.117463.

He, H., Hao, Z., Mladenoff, D., Shao, G., Hu, Y., Chang, Y., 2005. Simulating forest ecosystem response to climate warming incorporating spatial effects in north-eastern China. J. Biogeogr. 32, 2043-2056.http://dx.doi.org/10.1111/j.1365-2699.2005.01353.x.

Heiðarsson, L., Pukkala, T., 2011. Taper functions for lodgepole pine (Pinus contorta) and Siberian larch (Larix sibirica) in Iceland. Icel. Agric. Sci. 24, 3-11.

Hughes, M.K., Swetnam, T.W., Diaz, H.F., 2011. Dendroclimatology, progress and prospects. Developments in Paleoenvironmental Research, vol 11. Springer, Dordrecht.

Jiang, Y., Zhang, J., Han, S., Chen, Z., Setälä, H., Yu, J., Zheng, X., Guo, Y., Gu, Y., 2016. Radial Growth Response of Larix gmelinii to Climate along a Latitudinal Gradient in the Greater Khingan Mountains, Northeastern China. Forests 7, 295.http://dx.doi.org/10.3390/f7120295.

Kimmins, J.P., Blanco, J.A., Seely, B., Welham, C., Scoullar, K. 2008. Complexity in Modeling Forest Ecosystems; How Much is Enough? Forest Ecology and Management, 256(10), 1646-1658.

http://dx.doi.org/10.1016/j.foreco.2008.03.011

Kobak, K.I., Turcmnovich, I.Y., Kondrasiheva, N.Y., Schulze, E.-D., Schulze, W., Koch, H., Vygodskaya, N.N., 1996. Vulnerability and adaptation of the larch forest in eastern Siberia to climate change. Water, Air, Soil Pollut. 92, 119-127.http://dx.doi.org/10.1007/bf00175558.

Kozak, A., 2004. My last words on taper equations. For. Chron. 80, 507-515.http://dx.doi.org/10.5558/tfc80507-4.

Leng, W., He, H.S., Liu, H., 2008. Response of larch species to climate changes. Journal of Plant Ecology 1, 203-205.http://dx.doi.org/10.1093/jpe/rtn013.

Li, R., Weiskittel, A.R., 2010. Comparison of model forms for estimating stem taper and volume in the primary conifer species of the North American Acadian Region. Ann. For. Sci. 67, 302-302.http://dx.doi.org/10.1051/forest/2009109.

Lo, Y.-H., Blanco, J.A., Seely, B., Welham, C., Kimmins, J.P., 2010. Relationships between climate and tree radial growth in interior British Columbia, Canada. For. Ecol. Manage. 259, 932-942.http://dx.doi.org/10.1016/j.foreco.2009.11.033.

Marks, C.O., Muller-Landau, H.C., Tilman, D., 2016. Tree diversity, tree height and environmental harshness in eastern and western North America. Ecol. Lett. 19, 743-751.http://dx.doi.org/10.1111/ele.12608.

Meng, X., 2006. Forest Measurement. China Forestry Press, Beijing, China.

Messaoud, Y., Chen, H.Y.H., 2011. The Influence of Recent Climate Change on Tree Height Growth Differs with Species and Spatial Environment. PLoS ONE 6, e14691.http://dx.doi.org/10.1371/journal.pone.0014691.

Nigh, G., Smith, W., 2012. Effect of climate on lodgepole pine stem taper in British Columbia, Canada. Forestry 85, 579-587.http://dx.doi.org/10.1093/forestry/cps063.

Özçelik, R., Brooks, J.R., Jiang, L., 2011. Modeling stem profile of Lebanon cedar, Brutian pine, and Cilicica fir in Southern Turkey using nonlinear mixed-effects models. Eur. J. For. Res. 130, 613-621.http://dx.doi.org/10.1007/s10342-010-0453-5.

Parresol, B.R., Hotvedt, J.E., Cao, Q.V., 1987. A volume and taper prediction system for bald cypress. Can. J. For. Res. 17, 250-259.http://dx.doi.org/10.1139/x87-042.

Pauli, H., Gottfried, M., Dullinger, S., Abdaladze, O., Akhalkatsi, M., Alonso, J.L.B., Coldea, G., Dick, J., Erschbamer, B., Calzado, R.F., Ghosn, D., Holten, J.I., Kanka, R., Kazakis, G., Kollár, J., Larsson, P., Moiseev, P., Moiseev, D., Molau, U., Mesa, J.M., Nagy, L., Pelino, G., Puşcaş, M., Rossi, G., Stanisci, A.,

Syverhuset, A.O., Theurillat, J.-P., Tomaselli, M., Unterluggauer, P., Villar, L., Vittoz, P., Grabherr, G., 2012. Recent Plant Diversity Changes on Europe's Mountain Summits. Science 336, 353-355.http://dx.doi.org/10.1126/science.1219033.

Pinheiro, J., Bates, D., DebRoy, S., Sarkar, D., R-Core-Team, 2018. nlme: Linear and nonlinear mixed effects models. R package version 3.1-137. https://CRAN.R-project.org/package=nlme.

Pinheiro, J.C., Bates, D.M., 2000. Mixed-effects models in S and S-Plus. Springer-Verlag, New York.

Rojo, A., Perales, X., Sánchez-Rodríguez, F., Álvarez-González, J.G., Gadow, K.v., 2005. Stem taper functions for maritime pine (Pinus pinaster Ait.) in Galicia (Northwestern Spain). Eur. J. For. Res. 124, 177-186.http://dx.doi.org/10.1007/s10342-005-0066-6.

Sakamoto, Y., Ishiguro, M., Kitagawa, G., 1986. Akaike information criterion statistics. D. Reidel Publishing Company, Dordrecht, Netherlands.

Schneider, R., Franceschini, T., Fortin, M., Saucier, J.-P., 2018. Climate-induced changes in the stem form of 5 North American tree species. For. Ecol. Manage. 427, 446-455.http://dx.doi.org/10.1016/j.foreco.2017.12.026.

Schwarz, G., 1978. Estimating the dimension of a model. Ann. Stat. 6, 461-464.

Sharma, M., Parton, J., 2009. Modeling Stand Density Effects on Taper for Jack Pine and Black Spruce Plantations Using Dimensional Analysis. For. Sci. 55, 268-282.http://dx.doi.org/10.1093/forestscience/55.3.268.

Sharma, M., Zhang, S.Y., 2004. Variable-exponent taper equations for jack pine, black spruce, and balsam fir in eastern Canada. For. Ecol. Manage. 198, 39-53.http://dx.doi.org/10.1016/j.foreco.2004.03.035.

Skovsgaard, J.P., Vanclay, J.K., 2008. Forest site productivity: a review of the evolution of dendrometric concepts for even-aged stands. Forestry 81, 13-31.http://dx.doi.org/10.1093/forestry/cpm041.

Suvanto, S., Henttonen, H.M., Nöjd, P., Mäkinen, H., 2016a. Forest susceptibility to storm damage is affected by similar factors regardless of storm type: Comparison of thunder storms and autumn extra-tropical cyclones in Finland. For. Ecol. Manage. 381, 17-28.http://dx.doi.org/10.1016/j.foreco.2016.09.005.

Suvanto, S., Nöjd, P., Henttonen, H.M., Beuker, E., Mäkinen, H., 2016b. Geographical patterns in the radial growth response of Norway spruce provenances to climatic variation. Agric. For. Meteorol. 222, 10-20.http://dx.doi.org/10.1016/j.agrformet.2016.03.003.

Thomson, A.J., Barclay, H.J., 1984. Effects of thinning and urea fertilization on the distribution of area increment along the boles of Douglas-fir at Shawnigan Lake, British Columbia. Can. J. For. Res. 14, 879-

884.http://dx.doi.org/10.1139/x84-157.

Trincado, G., Burkhart, H.E., 2006. A Generalized Approach for Modeling and Localizing Stem Profile Curves. For. Sci. 52, 670-682.http://dx.doi.org/10.1093/forestscience/52.6.670.

Valentine, H.T., Gregoire, T.G., 2001. A switching model of bole taper. Can. J. For. Res. 31, 1400-1409.http://dx.doi.org/10.1139/x01-061.

Vonesh, E.F., Chinchilli, V.M., 1997. Linear and nonlinear models for the analysis of repeated measurements. Marcel Dekker, Inc., New York.

Wang, C., Gower, S.T., Wang, Y., Zhao, H., Yan, P., Bond‐Lamberty, B.P., 2001. The influence of fire on carbon distribution and net primary production of boreal Larix gmelinii forests in north‐eastern China. Global Change Biol. 7, 719-730.http://dx.doi.org/10.1046/j.1354-1013.2001.00441.x

Wang, H., Wang, W., Qiu, L., Su, D., An, J., Zheng, G., Zu, Y., 2012. Differences in biomass, litter layer mass and SOC storage changing with tree growth in Larix gmelinii plantations in Northeast China. Acta Ecol Sin 32, 833-843.http://dx.doi.org/10.5846/stxb201108311276.

Xu, H., 1998. Forests in Daxing'anling Mountains China. Science Press, Beijing, China.

Yang, Y., Huang, S., Trincado, G., Meng, S.X., 2009. Nonlinear mixed-effects modeling of variable-exponent taper equations for lodgepole pine in Alberta, Canada. Eur. J. For. Res. 128, 415-429.http://dx.doi.org/10.1007/s10342-009-0286-2.

Table 1. Summary statistics for the fitting and validation data

Variable	Fitting data				Validation data			
	Mean	SD	Min	Max	Mean	SD	Min	Max
No. of data points=8,583 (1,486 trees)					No. of data points=2,146 (372 trees)			
D(cm)	16.3	6.9	1.0	68.3	16.4	7.2	2.1	68.3
H(m)	15.3	4.1	2.0	43.0	15.3	4.3	3.2	41.9
MAT (°C)	-2.0	1.1	-3.6	-0.4	-2.0	1.1	-3.6	-0.4
MAP (mm)	437	75	361	558	437	75	361	558

D: diameter at breast height outside bark, *H*: total height, MAT: Mean annual temperature, MAP: Mean annual precipitation, Min: minimum, Max: maximum, SD: standard deviation.

Table 2. ANOVA of relative diameter (mean ± standard error) for different mean annual precipitation classes (MAPs) (<400 mm, 400 to 450 mm and >450 mm) for different relative height classes (*q* intervals of 0.1)

Relative height	< 400 mm		400 to 450 mm		>450 mm		*F*	*p*
	d/D	*N*	*d/D*	*N*	*d/D*	*N*		
$0<q\leq1$	0.660 ± 0.008^{a}	1493	0.767 ± 0.006^{b}	2982	0.808 ± 0.002^{c}	6256	213.2	<0.001
$0<q\leq0.1$	1.061 ± 0.006^{a}	202	1.168 ± 0.008^{b}	627	1.001 ± 0.001^{c}	2049	625.4	<0.001
$0.1<q\leq0.2$	0.972 ± 0.007^{a}	172	0.967 ± 0.002^{ab}	353	0.959 ± 0.002^{b}	486	4.4	0.012
$0.2<q\leq0.3$	0.888 ± 0.007^{a}	133	0.886 ± 0.003^{a}	256	0.825 ± 0.001^{b}	1054	255.8	<0.001
$0.3<q\leq0.4$	0.812 ± 0.007^{a}	135	0.833 ± 0.004^{b}	264	0.762 ± 0.002^{c}	438	123.0	<0.001
$0.4<q\leq0.5$	0.726 ± 0.007^{a}	139	0.761 ± 0.004^{b}	284	0.689 ± 0.001^{c}	936	190.4	<0.001
$0.5<q\leq0.6$	0.626 ± 0.007^{a}	150	0.685 ± 0.005^{b}	264	0.598 ± 0.002^{c}	638	186.9	<0.001
$0.6<q\leq0.7$	0.521 ± 0.008^{a}	127	0.589 ± 0.005^{b}	267	0.496 ± 0.003^{c}	445	140.6	<0.001
$0.7<q\leq0.8$	0.398 ± 0.007^{a}	150	0.460 ± 0.006^{b}	260	0.430 ± 0.003^{c}	200	27.1	<0.001
$0.8<q\leq0.9$	0.250 ± 0.006^{a}	162	0.283 ± 0.006^{b}	250	0.365 ± 0.017^{c}	10	11.5	<0.001
$0.9<q<1$	0.136±0.006	123	0.137±0.006	157	-	-	-	-

Note: The different superscript letters in the same row indicate significant differences among MAP classes; the same superscript letter in the same row indicate no significant differences among MAP classes (Tukey's HSD, $p < 0.05$).

Table 3. ANOVA of relative diameter (mean ± standard error) for different mean annual temperature classes (MATs) (<−3.0°C, −3.0 to −2.0°C and >−2.0°C) for different relative height classes (*q* intervals of 0.1)

Relative	< −3.0°C		−3.0 to −2.0°C		> −2.0 °C		*F*	*p*
height	*d/D*	*N*	*d/D*	*N*	*d/D*	*N*		
$0<q\leq1$	0.665 ± 0.009^{a}	1361	0.767 ± 0.006^{b}	2735	0.803 ± 0.002^{c}	6635	171.3	<0.001
$0<q\leq0.1$	1.050 ± 0.007^{a}	164	1.180 ± 0.009^{b}	573	1.004 ± 0.001^{c}	2141	665.5	<0.001
$0.1<q\leq0.2$	0.988 ± 0.006^{a}	169	0.968 ± 0.003^{b}	308	0.954 ± 0.002^{c}	534	25.6	<0.001
$0.2<q\leq0.3$	0.898 ± 0.006^{a}	132	0.891 ± 0.003^{a}	231	0.824 ± 0.001^{b}	1080	333.5	<0.001
$0.3<q\leq0.4$	0.830 ± 0.007^{a}	114	0.838 ± 0.004^{a}	248	0.759 ± 0.002^{b}	475	187.7	<0.001
$0.4<q\leq0.5$	0.733 ± 0.007^{a}	135	0.771 ± 0.004^{b}	255	0.688 ± 0.001^{c}	969	261.3	<0.001
$0.5<q\leq0.6$	0.637 ± 0.008^{a}	130	0.694 ± 0.005^{b}	243	0.596 ± 0.002^{c}	679	244.4	<0.001
$0.6<q\leq0.7$	0.527 ± 0.009^{a}	113	0.597 ± 0.005^{b}	244	0.496 ± 0.002^{c}	482	167.4	<0.001
$0.7<q\leq0.8$	0.400 ± 0.008^{a}	136	0.465 ± 0.007^{b}	237	0.425 ± 0.003^{c}	237	30.1	<0.001
$0.8<q\leq0.9$	0.251 ± 0.006^{a}	155	0.283 ± 0.007^{b}	239	0.299 ± 0.014^{a}	28	6.9	0.001
$0.9<q<1$	0.133 ± 0.007^{a}	113	0.136 ± 0.006^{a}	157	0.166 ± 0.008^{a}	10	0.9	0.413

Note: The different superscript letters in the same row indicate significant differences among MAT classes; the same superscript letter in the same row indicate no significant differences among MAT classes (Tukey's HSD, $p < 0.05$).

Table 4. Parameter estimates, and regression coefficients and standard errors (in parentheses) for Kozak (2004) model without (Eq. (1)) and with mean annual precipitation (MAP) and/or mean annual temperature (MAT) (Eqs. (2)–(4)), and with fixed- and random-effects parameters (with MAP and MAT incorporated) (Eq. (12)) plus an exponential variance function (varExp) and autoregressive error structure CAR(1)

	Eq. (1)	Eq. (2)	Eq. (3)	Eq. (4)	Eq. (12)	Eq. (12) with varExp and CAR(1) model
Parameters						
b_1	0.9687 (0.0084)	0.9658 (0.0082)	0.9703 (0.0082)	0.9699 (0.0082)	0.9671 (0.0142)	0.9885 (0.0179)
b_2	0.9759 (0.0053)	0.9771 (0.0052)	0.9750 (0.0051)	0.9752 (0.0051)	0.9612 (0.0070)	0.9471 (0.0081)
b_3	0.0445 (0.0074)	0.0444 (0.0073)	0.0451 (0.0072)	0.0450 (0.0072)	0.0586 (0.0095)	0.0649 (0.0111)
b_4	7.0916 (0.1319)	7.3330 (0.1311)	7.4603 (0.1300)	7.4630 (0.1300)	7.0610 (0.1115)	6.7590 (0.0974)
b_5	-1.1192 (0.2323)	-2.3000 (0.2404)	-1.9573 (0.2291)	-2.0330 (0.2385)	-4.1566 (0.3383)	-3.2684 (0.3174)
b_6	-10.4929 (0.3488)	-10.9100 (0.3453)	-9.9827 (0.3415)	-10.0500 (0.3473)	-7.5452 (0.3948)	-6.6081 (0.3580)
b_7	-0.6965 (0.0506)	5.6300 (1.1140)	3.9801 (1.0486)	4.3760 (1.1030)	11.2876 (1.2720)	7.5478 (1.2939)
b_8	0.0163 (0.0036)	0.0556 (0.0043)	0.0353 (0.0036)	0.0383 (0.0045)	0.0542 (0.0095)	0.0168 (0.0101)
b_9	15.1469 (0.4142)	13.5800 (0.4217)	14.5541 (0.4052)	14.4200 (0.4217)	12.0987 (0.4863)	11.3027 (0.4309)
b_{10}		0.0026 (0.0002)	0.1685 (0.0080)	0.1593 (0.0115)	0.2501 (0.0157)	0.2207 (0.0153)
b_{11}				0.0003 (0.0000)	-0.0002 (0.0000)	-0.0001 (0.0000)
Variance components						
σ^2	1.36189	1.32480	1.31077	1.29504	0.89750	0.30491
var(b_2)					0.00012	0.00004
var(b_8)					0.00154	0.00079
cov(b_2, b_8)					0.00032	0.00017
Variance structure						
δ						0.04227
Correlation structure						
ρ						0.45594
Goodness-of-fit						
AIC	27014.5	26784.8	26695.5	26596.3	25049.5	22651.0
BIC	27085.1	26862.4	26773.2	26681.0	25155.4	22771.0
logLik	-13497.3	-13381.4	-13346.8	-13286.1	-12509.8	-11308.5

Table 5. Evaluation statistics of nonlinear mixed-effects (NLME) models and models with and without mean annual precipitation (MAP) and mean annual temperature (MAT) for analyzed variable-form taper Kozak (2004) model

Model	Fitting				Validating		
	R^2	RMSE	MAE	MPRB(%)	RMSE	MAE	MPRB(%)
Eq. (1)	0.9790	1.1667	0.7230	5.4828	1.0407	0.6969	5.2848
Eq. (2)	0.9795	1.1511	0.7028	5.3302	1.0176	0.6734	5.1068
Eq. (3)	0.9800	1.1385	0.6930	5.2559	1.0091	0.6684	5.0683
Eq. (4)	0.9813	1.1274	0.6829	5.1546	1.0037	0.6575	5.0521
Eq. (12) with varExp and CAR(1) model	0.9888	1.0712	0.6652	5.0444	0.9699	0.6256	4.6816

Table 6. Root mean squared error (RMSE), mean absolute error (MAE) and mean percentage of relative bias (MPRB) (%) for the predictions of diameter outside bark for validation data for nonlinear mixed-effects (NLME) models and models with and without mean annual precipitation (MAP) and mean annual temperature (MAT) for analyzed Kozak (2004) model

Relative height	N	Kozak (2004)			Kozak (2004) with MAP and MAT			Eq. (12) with varExp and CAR(1) model		
		RMSE	MAE	MPRB(%)	RMSE	MAE	MPRB(%)	RMSE	MAE	MPRB(%)
0-0.1	578	**1.2966**	0.7455	4.0039	1.3231	0.7617	4.0907	1.3501	**0.6825**	**3.6656**
0.1-0.2	187	0.5814	0.3676	2.5412	0.5871	0.3757	2.5969	**0.5481**	**0.3664**	**2.5326**
0.2-0.3	281	0.7602	0.5608	4.0495	0.7224	0.5400	3.8993	**0.5161**	**0.4826**	**3.4851**
0.3-0.4	160	0.9918	0.7499	5.4795	0.8854	0.6673	4.8762	**0.8678**	**0.6046**	**4.4181**
0.4-0.5	295	1.0161	0.7078	6.0801	0.8938	0.6328	5.4364	**0.8024**	**0.5907**	**5.0747**
0.5-0.6	206	0.9542	0.7131	6.4540	0.8796	0.6283	5.6862	**0.8050**	**0.6191**	**5.6032**
0.6-0.7	184	1.2005	0.9059	10.0940	1.0858	0.7965	8.8757	**0.9000**	**0.7411**	**8.2584**
0.7-0.8	127	**1.2064**	**0.8459**	**10.7765**	1.2421	0.8722	11.1122	1.2746	0.9127	11.6278
0.8-0.9	84	**0.9602**	**0.7279**	**18.8906**	1.0094	0.7389	19.1756	1.0594	0.7386	19.1686
0.9-1.0	44	**0.8316**	**0.6223**	**40.1463**	0.8897	0.6363	41.0484	1.0201	0.7055	45.5183
Overall	2146	1.0407	0.6969	5.2848	1.0037	0.6575	5.0521	**0.9699**	**0.6256**	**4.6816**

Note: Numbers shown in bold indicate the lowest errors of each criteria for three models in diameter prediction for each relative height (q).

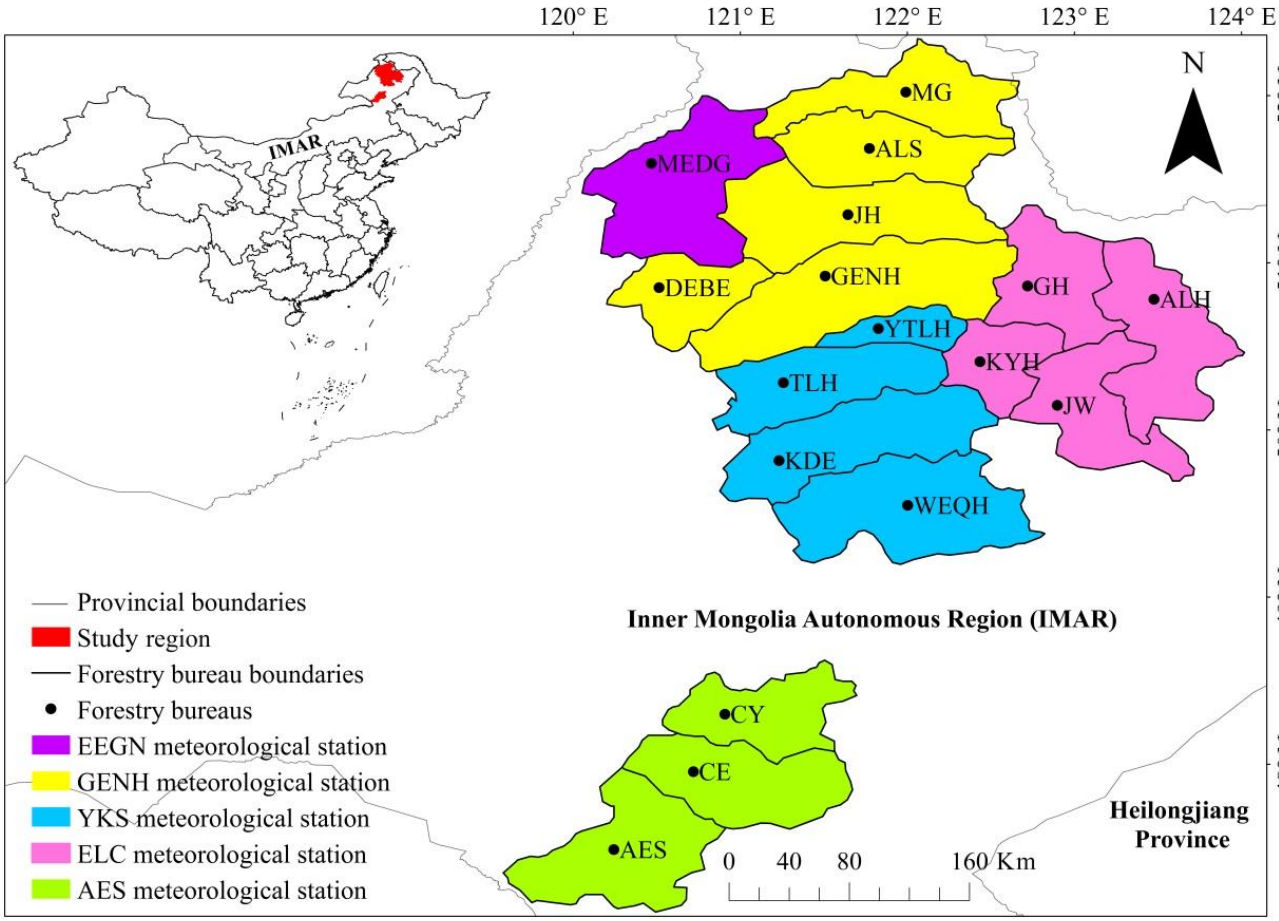

Figure 1. Location of the study region in the Greater Khingan Mountains of Inner Mongolia, northeast China and 17 Forestry Bureaus belonged to five meteorological stations.

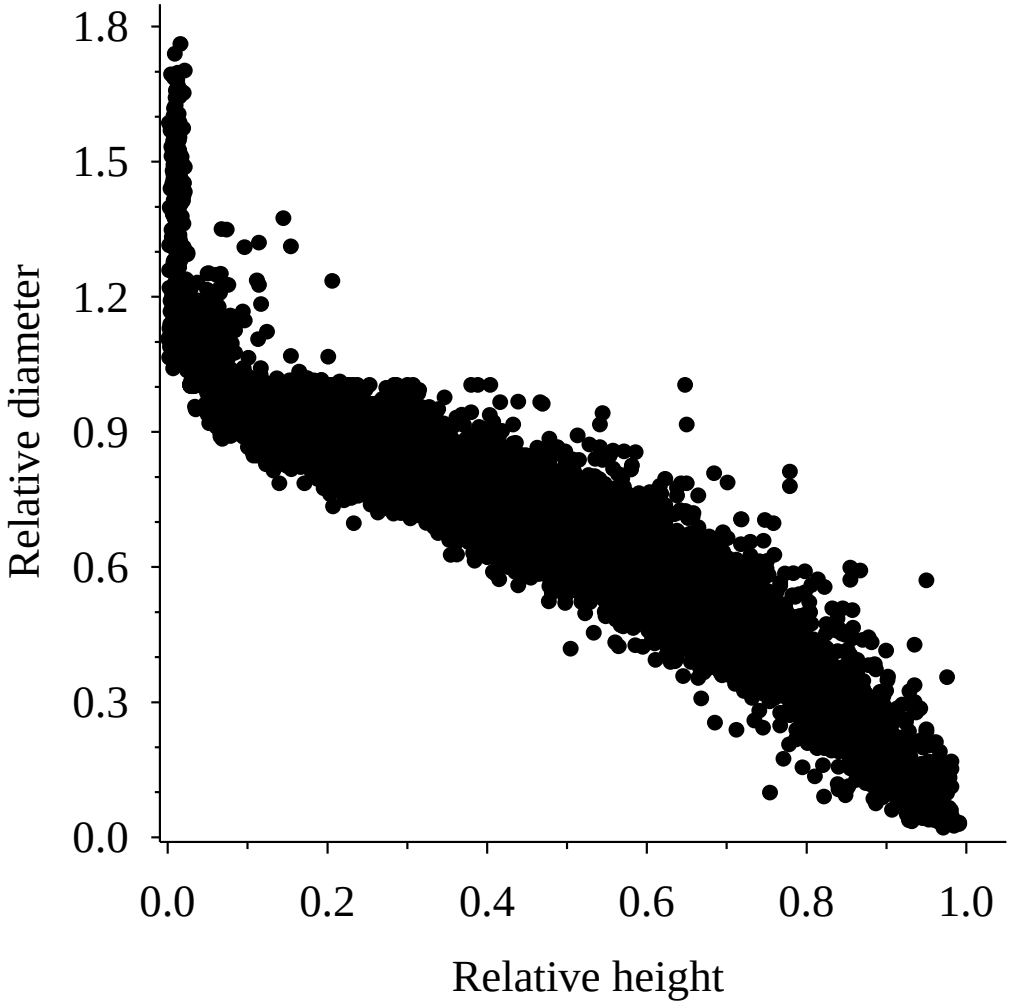

Figure 2. Scatterplot between the relative height (*h*/*H*) and relative diameter (*d*/*D*).

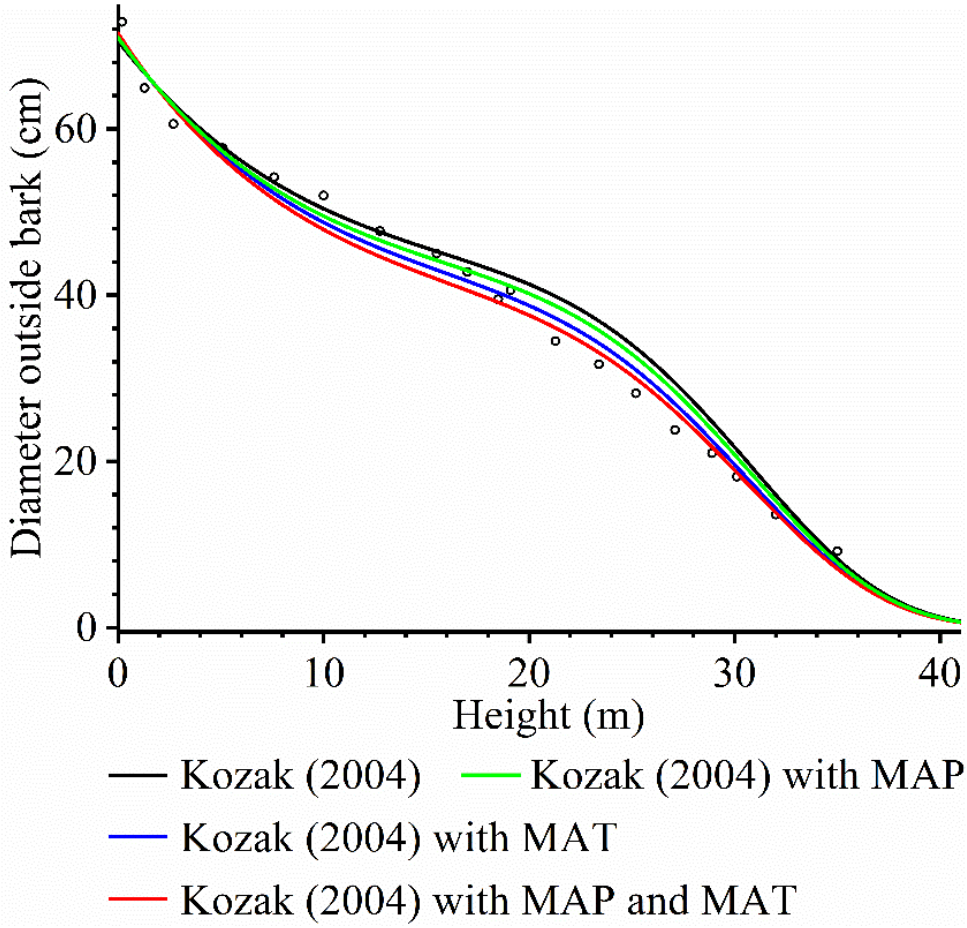

Figure 3. Predicted diameter over height (an example for *Larix gmelinii* (*D*=64.9 cm, *H*=37.2 m, MAT=−2.3°C and MAP=441.4 mm)) using the Kozak (2004) model (black line), Kozak (2004) model with mean annual precipitation (MAP) (green line), Kozak (2004) model with mean annual temperature (MAT) (blue line), and Kozak (2004) model with MAP and MAT (red line). The four color codes represent the four different taper models. The hollow dots represent the measured value of the upper-stem diameter at the corresponding height along the tree bole.

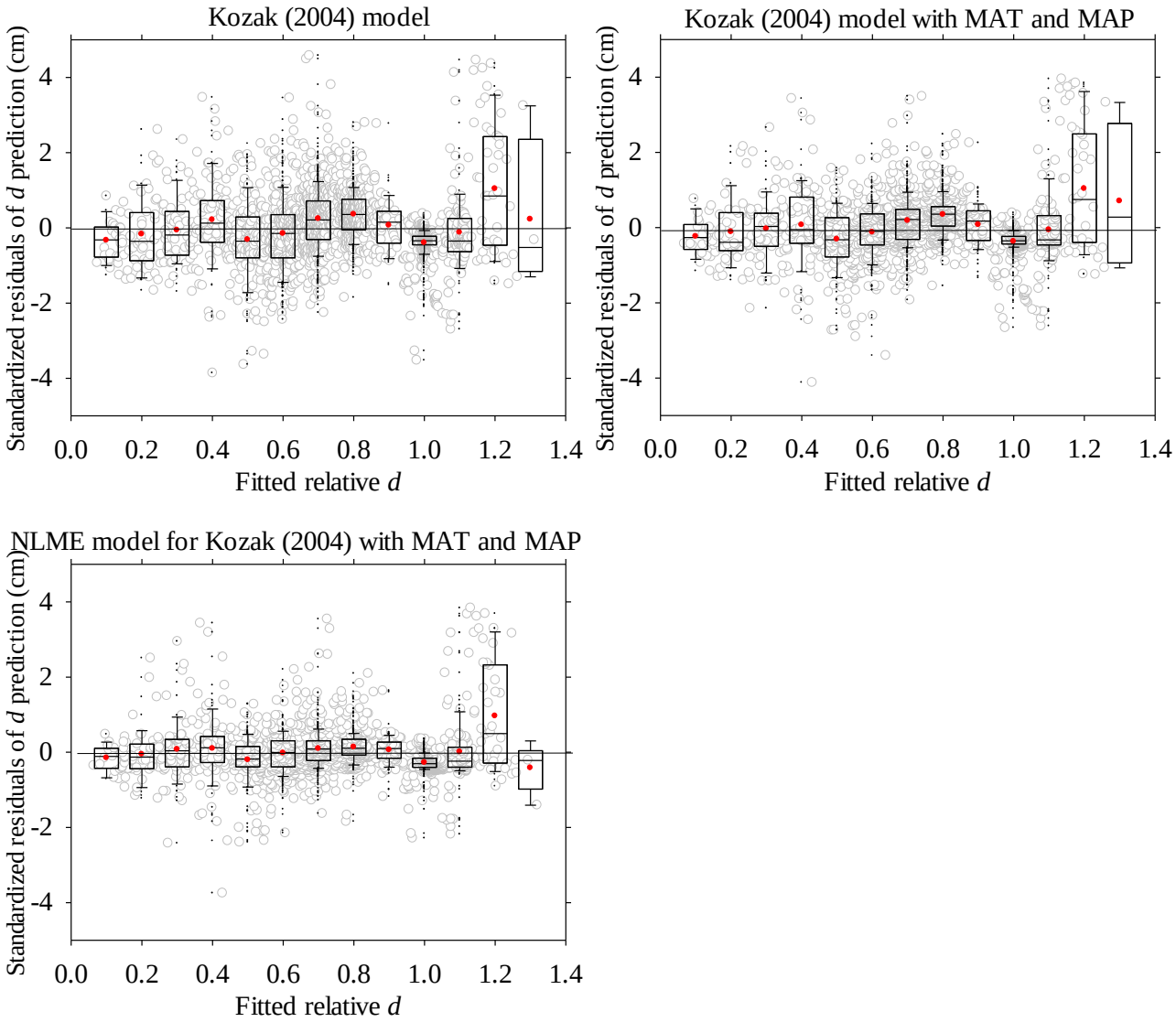

Figure 4. Standardized residuals of diameter for the Kozak (2004) model, Kozak (2004) model with mean annual precipitation (MAP) and mean annual temperature (MAT) incorporated, and with fixed- and random-effects parameters (with MAT and MAP incorporated) plus an exponential variance function and autoregressive error structure CAR(1), where four randomly selected prior measured upper stem diameters above ground from sample tree were used for estimating random-effects parameters and then for making tree-specific diameter calibrations. Box plots represent the mean (red dot), median (middle line), the 25th (bottom of box) and 75th quartile (top of box), maximum (top whisker), minimum (bottom whisker) and outliers (black dot) standardized residual of diameter for each relative height class.